Nuclear Instruments and Methods in Physics Research B59/60 (1991) 1313–1316
North-Holland

Photoluminescence and structural characterization of MeV erbium-implanted silica glass

A. Polman, D.C. Jacobson, A. Lidgard [1] and J.M. Poate
AT&T Bell Laboratories, 600 Mountain Avenue, Murray Hill, NJ 07974, USA

G.W. Arnold
Sandia National Laboratories, Albuquerque, NM 87185, USA

Suprasil glass (amorphous SiO_2) has been implanted with 2.9 MeV Er ions at fluences of 3.4×10^{15} and 3.4×10^{16} ions/cm^2. Photoluminescence spectra of implanted samples show a clear luminescent transition around $\lambda = 1.54$ μm, corresponding to an intra-4f transition of Er^{3+}. Fluorescence decay times are in the range 1–8 ms, depending on implantation fluence and annealing treatment. UV absorption and IR reflection spectroscopy are employed to characterize beam-induced defects in the silica network. The results indicate that defects in the silica network play an important role in the energy transfer processes in the Er : silica system.

1. Introduction

Optical doping of insulators and semiconductors using ion beams is a new and unexploited area in the field of ion–solid interactions. Until today, the limited number of investigations concerns implantation of Si [1–3], III–V semiconductors [3–5], $LiNbO_3$ [6] and silica glass [7], with rare-earth elements such as Er, Nd and Yb. These elements have the interesting property that, when incorporated with trivalent charge state in a solid host, their electronic energy levels differ only slightly from those of the free ion. This is a result of the fact that the 4f orbitals of trivalent rare-earths are effectively shielded by the outer lying closed $5s^2$ and $5p^6$ shells. The Er : silica-glass system is of particular interest because Er has an intra-4f transition at a wavelength (λ) of 1.54 μm, coinciding with the low-loss window of standard silica-based telecommunications fiber.

Recently, we have shown that it is possible to incorporate optically active Er in thin silica glass films on a Si substrate using a MeV ion beam [7]. In this article we concentrate on MeV Er implantation in Suprasil silica glass. This material is available in bulk form, which enables ultraviolet (UV) absorption and infrared (IR) reflection spectroscopy studies to be made in order to investigate radiation-induced changes in the silica network. These data are correlated with a photoluminescence study in which the intra-4f transitions in the Er : silica system are investigated.

[1] On leave from Dept. of Physics, Royal Inst. of Technology, Stockholm, Sweden.

2. Experimental

High-purity fused silica glass (amorphous SiO_2) samples, commercially known as Suprasil 1, were implanted on one side with 2.9 MeV Er ions. Implantation was done at room temperature and the fluences were either 3.4×10^{15} or 3.4×10^{16} ions/cm^2. The Er concentration profiles as a function of depth were determined using Rutherford backscattering spectrometry. The as-implanted profile was nearly Gaussian shaped with the peak at 1.04 μm depth and a full width at half maximum (FWHM) of 0.46 μm. The Er peak concentration was 0.1 at.% or 1.0 at.% for low- and high-fluence implanted samples, respectively. Thermal annealing for one hour at 900 °C was carried out on some samples using a standard tube-furnace at a base pressure below 10^{-6} Torr. Annealing did not lead to any measurable diffusion of Er.

Photoluminescence (PL) measurements were performed at room temperature, using the $\lambda = 488$ nm line of an Ar^+ laser as a pump source. Time-resolved fluorescence decay measurements were performed at $\lambda = 1.536$ μm. The 850 μs FWHM excitation pulse was obtained by mechanical chopping and had rise and fall times of 150 μs. Decay data were collected using a digitizing oscilloscope. Optical absorption measurements were performed using a dual-beam Cary 23 spectrophotometer and all measurements were performed against an unimplanted sample in the reference beam. IR reflection spectroscopy was performed in the lattice-mode region of the infrared using a Nicolet 60 SX FTIR instrument.

Elsevier Science Publishers B.V. (North-Holland)

3. Results

3.1. Photoluminescence

Fig. 1 shows a photoluminescence spectrum for a sample implanted with 3.4×10^{15} ions/cm^2 and annealed at 900 °C. Clearly, a luminescence peak is observed around $\lambda = 1.54$ μm. This wavelength coincides with the wavelength of the transitions between the first excited manifold $^4I_{13/2}$ and the $^4I_{15/2}$ ground manifold of Er^{3+} ($4f^{11}$) [8]. The PL peak is composed of a main peak $\lambda = 1.536$ μm and a side peak with somewhat lower intensity at $\lambda = 1.552$ μm. A spectrum for a sample implanted at 10 times higher fluence and annealed at 900 °C is also shown in fig. 1. In the figure, its amplitude is reduced by a factor 9. The double-peak structure is less pronounced and the spectrum is somewhat broader. Spectra for unannealed samples were roughly similar to those for the annealed samples in fig. 1, apart from their intensity. Table 1 lists the integrated PL intensities for all implanted samples. It can be seen that thermal annealing increases the PL intensities by a factor 4 or 7 for low- and high-fluence implants respectively. For the annealed samples the integrated PL intensities are proportional to the Er fluence.

Time-resolved measurements of the fluorescence decay showed a single-exponential decay for all samples [9]. The 1/e times range from 1–8 ms and are listed in table 1. As can be seen, thermal annealing increases the decay time. When the Er concentration is increased, the decay time becomes shorter.

3.2. UV absorption

Fig. 2 shows a compilation of optical absorption spectra of samples implanted with 3.4×10^{15} ions/cm^2

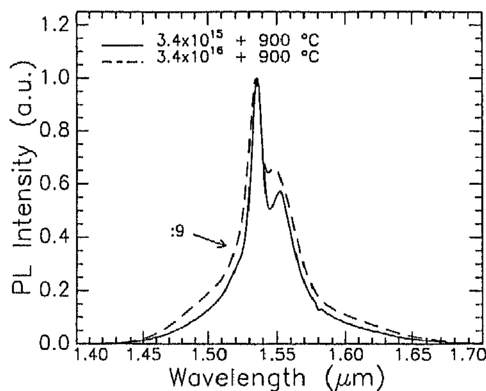

Fig. 1. Room-temperature photoluminescence spectra for silica glass implanted with 2.9 MeV Er at two different fluences (indicated in the figure) and annealed at 900 °C for 1 h. Both measurements were performed using the same pump power ($\lambda = 488$ nm).

Table 1
Integrated PL intensities and fluorescence decay times of Er-implanted silica samples

Fluence [ions/cm^2]	Annealing	PL intensity [a.u.]	Decay time [ms]
3.4×10^{15}	–	1.00 ± 0.03	3.2 ± 0.1
	900 °C, 1 h	3.5 ± 0.1	7.9 ± 0.2
3.4×10^{16}	–	5.3 ± 1.1	1.2 ± 0.1
	900 °C, 1 h	34.4 ± 1.9	5.7 ± 0.1

(as-implanted and implanted + annealed at 900 °C) and a sample implanted with 3.4×10^{16} ions/cm^2 (as-implanted only). For the as-implanted samples an absorption structure is found between $\lambda = 185$ and 280 nm. Absorption in this wavelength region is well-documented and has been identified to correspond to two types of defects: the E′-center (an O-vacancy opposite an electron in a dangling Si sp^3 orbital, in the spectrum centered around 215 nm) [10] and the B_2-center (presumably related to an O-vacancy which has trapped two electrons, at about 245 nm) [11]. Both defects are known to be mainly produced as a result of the collisional component of the ion-energy deposition process.

As is evident from fig. 2, the high-fluence implant yields a higher absorption than the low-fluence implant. This indicates that there is no saturation in the concentration of beam-induced point defects for 2.9 MeV Er fluences up to ~ 10^{16} ions/cm^2. For this fluence the number of ion-induced displacements per atom (dpa), estimated using TRIM [12], amounts to ~ 35 dpa. After annealing at 900 °C, the low-fluence implanted sample shows no noticeable absorption in the 185–400 nm wavelength region indicating that all E′ and B_2 centers are annealed out. Indeed, it has been observed earlier that point defects of the type considered here anneal out at temperatures of 400 °C and higher [13].

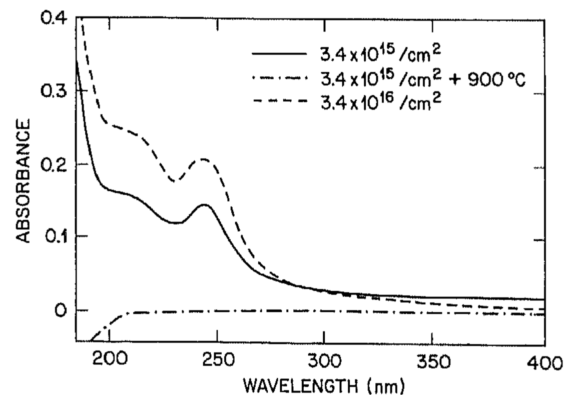

Fig. 2. Optical absorption measurements for silica glass implanted with 3.4×10^{15} Er ions/cm^2 (as-implanted and implanted + annealed) and 3.4×10^{16} Er ions/cm^2 (as-implanted).

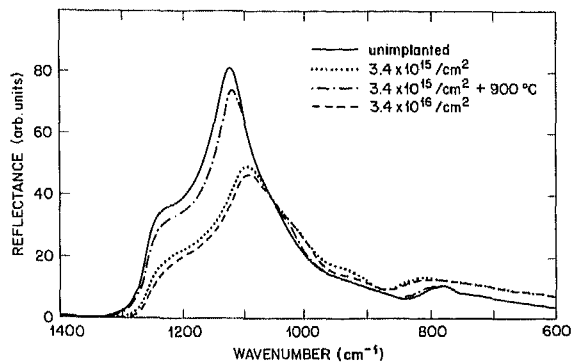

Fig. 3. Infrared reflection measurements for silica glass implanted with 3.4×10^{15} Er ions/cm^2 (as-implanted and implanted + annealed) and 3.4×10^{16} Er ions/cm^2 (as-implanted). A spectrum for an unimplanted sample is shown for reference.

Absorption measurements were also performed in the wavelength region around the luminescent transition at $\lambda = 1.54$ μm and no noticeable defect-related absorption was found. This is an important finding for future use of Er-implanted Suprasil glass in optical devices. Another concern has been that high concentrations of Er might lead to colloid formation and result in undesired light-scattering. There is no evidence for colloidal absorption in the data of fig. 2.

3.3. IR reflection

Fig. 3 shows IR reflection spectra for samples implanted at 3.4×10^{15} ions/cm^2 (as-implanted and implanted + annealed at 900 °C) and 3.4×10^{16} ions/cm^2 (as-implanted only). A spectrum for an unimplanted sample is also shown and shows a peak at around 1128 cm^{-1} corresponding to the Si–O–Si stretch vibration [14]. The production of damage by the ion beam causes a shift of this peak to lower wavenumber. This has been observed earlier and is thought to be due to an increase in the mean Si–O bond length and a decrease in the mean equilibrium bridging angle (normally 144°) [15]. Also, a small damage band is observed around 1015 cm^{-1}. This mode is believed to be due to dangling Si–O groups [14]. It is interesting to note that only a slight difference is observed between the spectra for the low- and high-fluence as-implanted samples. This suggests that a saturation in network distortion occurs above a 2.9 MeV Er fluence on the order of $\sim 10^{15}$ ions/cm^2.

4. Discussion

All implanted samples show a luminescence peak around $\lambda = 1.54$ μm. For the high-fluence annealed implant, the double-peak structure in the PL spectra becomes less apparent and the spectrum becomes wider, which indicates a wider configurational distribution of Er sites at high concentration. Although the UV absorption and IR reflection measurements of the as-implanted samples clearly show the presence of beam-induced defects and distortions in the silica network, it appears that these defects do not prevent the Er from being incorporated on an optically active site. For Er to be optically active, it needs to be incorporated in its trivalent state. This possibly takes place through an ionic bonding to nonbridging oxygen ions in the silica network. Thermal annealing might stimulate formation of these Er–O bonds, which can partly explain the increase in luminescence intensity upon annealing.

Thermal annealing also increases the fluorescence decay time of implanted samples (see table 1). This suggests that in as-implanted samples the excited state is partly depleted through nonradiative paths. These paths are presumably defect-related and hence a thermal treatment, which (partly) anneals out the corresponding defects (see UV and IR spectra), results in a longer decay time. The decay time for the unannealed low-fluence implanted sample is significantly longer than for the unannealed high-fluence implanted sample (5.7 vs 1.2 ms). For annealed samples, the decay times for high- and low-fluence implanted samples are also different. This suggests that concentration-quenching effects, involving energy transfer processes between rare-earth ions [8], might play a role at concentrations of at least ~ 1 at.%.

An increase in PL decay time also results in an increased PL intensity. To first order, assuming a simple process involving two different probabilities for radiative and non-radiative $^4I_{13/2} \to {}^4I_{15/2}$ transitions, the PL intensity would be proportional to the measured decay time of the $^4I_{13/2}$ excited state [9]. Comparing the data in table 1 for unannealed and annealed samples at a given Er fluence, it is seen that the PL intensity increases more than linearly with decay time. This indicates that thermal annealing, apart from reducing the defect concentration, also increases the total number of optically active Er ions. More complicated processes, e.g., involving annealing of defect states above the $^4I_{13/2}$ level might also play a role.

5. Conclusion

2.9 MeV Er implanted Suprasil glass shows a strong luminescent transition around $\lambda = 1.54$ μm corresponding to an intra-4f transition of Er^{3+}. Fluorescence decay times are in the range 1–8 ms. Beam-induced defects in as-implanted samples can be identified using UV and IR spectrosopy. Thermal annealing reduces the defect concentration and increases the luminescence decay time. This indicates that defects in the silica network play an important role in the energy transfer processes

within the Er : silica system. An increase in PL intensity is observed after annealing and is attributed to the increase in decay time as well as an increase in the number of optically active Er^{3+} ions. This correlation between UV absorption, IR reflection and luminescence measurements enables us to converge results on radiation damage in glass and optical activity of implanted Er into a clear picture.

Acknowledgement

The work of G.W. Arnold was supported by the U.S. Department of Energy under contract number DE-AC04-76DP00789.

References

[1] Y.S. Tang, K.C. Heasman, W.P. Gillin and B.J. Sealy, Appl. Phys. Lett. 55 (1989) 432.
[2] D. Moutonnet, H. l'Haridon, P.N. Favennec, M. Salvi, M. Gauneau, F. Arnoud d'Avitaya and J. Chroboczek, Mater. Sci. Eng. B4 (1989) 75.
[3] H. Ennen, J. Schneider, G. Pomrenke and A. Axmann, Appl. Phys. Lett. 43 (1983) 943.
[4] G.S. Pomrenke, H. Ennen and W. Haydl, J. Appl. Phys. 59 (1986) 601.
[5] G. Aszodi, J. Weber, Ch. Uihlein, L. Pu-Lin, H. Ennen, U. Kaufmann, J. Schneider and J. Windscheif, Phys. Rev. B31 (1985) 7767.
[6] R. Brinkmann, C. Buchal, S. Mohr, W. Sohler and H. Suche, Proc. Integr. Phot. Res. Conf., Hiltonhead, SC, USA, 1990.
[7] A. Polman, A. Lidgard, D.C. Jacobson, P.C. Becker, R.C. Kistler, G.E. Blonder and J.M. Poate, Appl. Phys. Lett. 57 (1990) 2859.
[8] S. Hufner, Optical Spectra of Transparent Rare-Earth Compounds (Academic Press, New York, 1978).
[9] A. Polman, D.C. Jacobson and J.M. Poate, to be published.
[10] See, e.g.; F.J. Feigl, W.B. Fowler and K.L. Yip, Solid State Commun. 14 (1974) 225.
[11] G.W. Arnold, IEEE Trans. Nucl. Sci. NS-20 (1973) 220.
[12] J.P. Biersack and L.J. Haggmark, Nucl. Instr. and Meth. 174 (1980) 257.
[13] U. Katenkamp, H. Karge and R. Prager, Radiat. Eff. 48 (1980) 31.
[14] G.W. Arnold, The Physics of MOS Insulators, eds. G. Lucovsky, S.T. Pantelides and F.L. Galeneer (Pergamon, New York, 1980) p. 112.
[15] G.E. Walrafen and M.S. Hokmabadi, in: Structure and Bonding in Noncrystalline Solids (Plenum, New York, 1986) p. 185.